F4TCNQ on Cu, Ag, and Au as prototypical example for a strong organic acceptor on coinage metals

Gerold M. Rangger,[1] Oliver T. Hofmann,[1] Lorenz Romaner,[1,2] Georg Heimel,[3] Benjamin Bröker,[3] Ralf-Peter Blum,[3] Robert L. Johnson,[4] Norbert Koch,[3] and Egbert Zojer[1]

[1]*Institut für Festkörperphysik, Technische Universität Graz, A-8010 Graz, Austria*

[2]*Department of Material Physics, University of Leoben, A-8700 Leoben, Austria*

[3]*Institut für Physik, Humboldt-Universität zu Berlin, D-12389 Berlin, Germany*

[4]*Institut für Expermentalphysik, Universität Hamburg, D-22761 Hamburg, Germany*

(Received 23 December 2008; revised manuscript received 18 February 2009; published 8 April 2009)

Metal work-function modification with the help of organic acceptors is an efficient tool to significantly enhance the performance of modern state-of-the-art organic molecular electronic devices. Here, the prototypical organic acceptor 2,3,5,6-tetrafluoro-7,7,8,8-tetracyanoquinodimethane, F4TCNQ, is characterized on Ag(111), Au(111), and Cu(111) metal surfaces by means of density-functional theory calculations. Particular attention is paid to charge-transfer processes at the metal-organic interface; a subtle balance between charge forward and backward donations in combination with a strong adsorption-induced geometry change are found to be responsible for the observed increase in the system work function. A larger effect is obtained for the metals with larger initial work function. Interestingly, this results in similar charge-injection barriers from the substrate metal into an organic semiconductor deposited on top of the F4TCNQ layer. The impact of the F4TCNQ packing density of the electronic properties of the interface is also addressed. Comparing the calculated energy-level alignments and work-function modifications to experimental data from ultraviolet photoelectron spectroscopy yields good agreement between experiments and simulations.

DOI: 10.1103/PhysRevB.79.165306 PACS number(s): 73.30.+y, 71.15.Mb, 31.10.+z, 68.43.−h

I. INTRODUCTION

Physical and chemical processes taking place at the interface between metals and organic molecules have attracted considerable attention in recent years[1–7] since such junctions can crucially determine the performance of organic (opto)electronic devices.[8–13] Several strategies have been developed to tune the alignment between the metal Fermi level and the molecular states and, thus, to facilitate carrier-injection across metal-organic interfaces. These include the application of polar, covalently bound self-assembled monolayers,[14–22] redox doping of the organic layers,[23,24] or the deposition of (sub)monolayers of strong electron acceptors[25–29] (or donors[1,13,30,31]), which form charge-transfer complexes with the underlying metal.[32–38] The latter are of particular relevance for the present study.

Usually, when apolar molecules physisorb on clean metal surfaces, the respective work functions are reduced by Pauli repulsion.[2] For example, a work-function decrease in the range of 0.38 to 0.42 eV has been reported for the adsorption of the noble gas Ar on the (111) surfaces of Cu, Ag, and Au.[39] The decrease is nearly twice as large for (inert) alkane chains on Au, Ag, and Pb.[40] This phenomenon is detrimental for the injection of holes from a metal electrode into an organic semiconductor. It can, however, be avoided by depositing an interfacial (sub)monolayer consisting of molecules which induce electron transfer from the metal to the organic adsorbate. This can be achieved by depositing strong organic acceptors.[2,25,26,32,36] A particularly potent and in the meantime "prototypical" example for such an acceptor is 2,3,5,6-tetrafluoro-7,7,8,8-tetracyanoquinodimethane (F4TCNQ). It has been shown by photoelectron spectroscopy that charge is transferred from Au,[26] Ag,[29] and Cu surfaces[37] to F4TCNQ. This could be used to reduce the hole-injection barriers (HIB) into organic semiconductor molecules deposited on top of the F4TCNQ monolayers. In fact, even a continuous tuning of the HIB over a wide range could be achieved by changing the F4TCNQ coverage.[26,29] We have shown recently[37] by a combined theoretical and experimental study for submonolayers of F4TCNQ on Cu(111) that the actual charge redistribution at the interface is much more complex than one might infer merely on the basis of photoelectron data.

Here, we discuss the involved processes in considerably more detail for several related systems. First, we focus on a densely packed F4TCNQ layer on Ag(111); this substrate metal is chosen as the "working horse" of the present contribution for reasons discussed below. Moreover, we describe, how changing the packing density of the adsorbate affects the electronic structure of the interface and discuss a possible reason why depolarization in densely packed F4TCNQ layers is only of minor significance. Subsequently, the role of the substrate metal for the interfacial charge transfer, energy-level pinning, and the resulting work-function change is addressed. Finally, the results of the calculations are compared to experimental data with a focus on measurements performed on Ag (111) surfaces.

II. METHODOLOGY

A. Computational methodology

The calculations presented here are based on density-functional theory (DFT), using the generalized gradient approximation (GGA). The plane-wave-based code Vienna *ab initio* simulation package (VASP) (Refs. 41 and 42) is applied

in the repeated slab approach using the PW91 functional.[43,44] Two different Monkhorst-Pack[45] k-point grids $(4\times4\times1)$ and $(3\times3\times1)$ are used depending on the size of the unit cells, together with a second-order Methfessel-Paxton occupation scheme[46] (broadening of 0.2 eV). All calculations were done in a non-spin-polarized manner. In all cases discussed here, five layers of metal represent the metal substrate and a vacuum gap of more than 20 Å separates the slabs in z direction. All atoms of the molecule as well as of the two top metal layers were fully relaxed using a damped molecular-dynamics scheme until the remaining forces were smaller than 0.01 eV/Å. To obtain the density of states (DOS) projected onto the molecular monolayer [i.e., the molecular density of states (MDOS)], each Kohn-Sham orbital was projected onto spherical harmonics inside spheres around each atom. Subsequently, the DOS was weighted according to the contributions of that atomic orbital and all nonmetallic contributions were summed up. For the special charge conserving projections of the DOS of the system onto the bands derived from the molecular orbitals (MOs) calculated without the metal, we applied the atomic-orbital-based code SIESTA.[47] A more detailed description of the methodology applied in the SIESTA calculations can be found in Ref. 48. Despite the methodological differences between VASP and SIESTA, the deviations between the obtained DOSs of the system are negligible.[49] XCRYSDEN (Ref. 50) was used to plot unit cells and three-dimensional (3D) charge rearrangements. GAUSSIAN03 (Ref. 51) was used to obtain the isodensity representations of the molecular orbitals. The double-zeta polarized basis set 6-31G(d,p) (Refs. 52 and 53) was employed in conjunction with the B3LYP exchange-correlation functional.[54,55]

B. Structure of the systems

The chemical structure of F4TCNQ is shown in Fig. 1(a). It is characterized by four electron withdrawing –CN groups at its extremities and four highly electronegative F atoms attached to the central ring. Moreover, in its charge neutral state, the central ring is distorted toward a quinoidal structure, which is known to further promote charge transfer through aromatic stabilization in the charged state.[56] When adsorbed on the (111) surfaces of Au and Ag, the F4TCNQ molecules were arranged in two different surface unit cells corresponding to dense (monolayer) and loose (submonolayer) packing. The former is shown in Fig. 1(b) and corresponds to a $\begin{pmatrix} 4 & -1 \\ 4 & 0 \end{pmatrix}$ surface unit cell. It has been observed experimentally for a F4TCNQ monolayer on Au(111) by low-temperature scanning tunneling microscopy (STM).[57] It is at least reasonable to assume a similar structure for densely packed F4TCNQ on Ag(111), considering the virtually identical dimensions of the surface unit cells of Au(111) and Ag(111). To the best of our knowledge, no low-energy electron-diffraction (LEED) or low-temperature STM data that would allow an unambiguous determination of the adsorption structure are available for F4TCNQ on Ag(111). For studying loosely packed layers, a $(3\sqrt{3}\times5)$ cell as shown in Fig. 1(c) has been chosen. In the densely packed monolayer, the long molecular axes are parallel to the $\langle1\bar{1}0\rangle$ direction

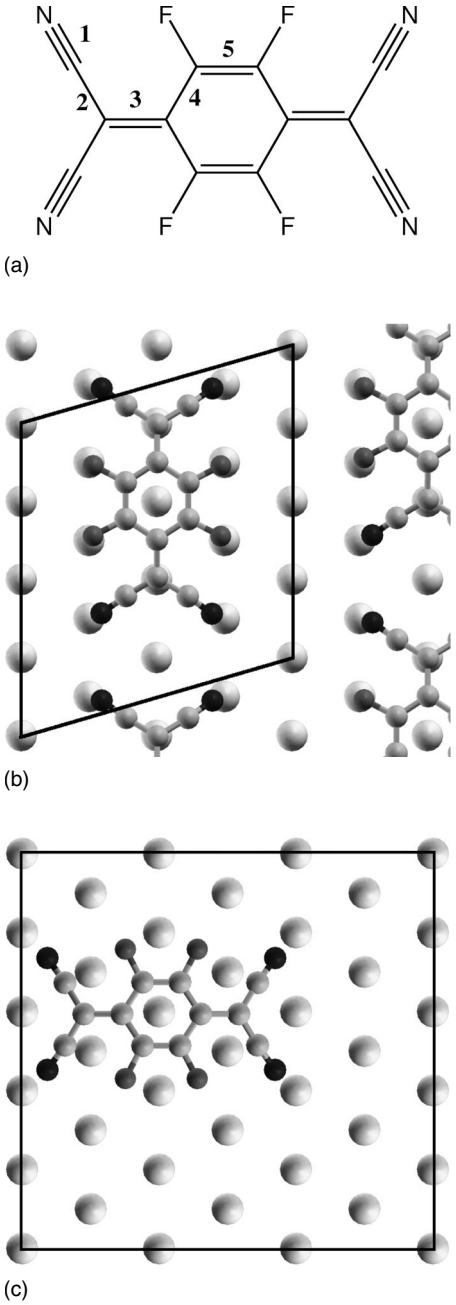

FIG. 1. (a) Chemical structure of F4TCNQ. (b) Experimentally suggested unit cell for F4TCNQ on Au(111), which is used here also on Ag(111). The long molecular axis of F4TCNQ is parallel to the $\langle1\bar{1}0\rangle$-direction. (c) Loosely packed F4TCNQ molecules on Ag(111) in analogy to the structure on Cu(111) as studied in Ref. 37. The long molecular axis is parallel to the $\langle11\bar{2}\rangle$ direction. Only the top metal layer and the molecule are shown for reasons of clarity.

consistent with the above mentioned experiments.[57] In loosely packed layers, the molecular orientation is not known. Therefore, we have first aligned the molecules along the $\langle11\bar{2}\rangle$ direction[37] and then rotated them in steps of 30 degrees until they pointed in the $\langle1\bar{1}0\rangle$ direction.[58] Maximum variations in the induced work-function change were only around 0.05 eV. Therefore, to ease comparison with the data

in Ref. 37, molecules aligned parallel to the $\langle 11\bar{2}\rangle$ direction will be discussed in the following for low coverages.

For the Cu(111) surface, only the loose-packing geometry is studied, as the Cu lattice constant is by about 14% shorter than that of Ag and Au. This rules out adopting the experimental unit cell found on Au(111) (vide supra), as this would result in unrealistically small interatomic distances on Cu(111). The nitrogen-nitrogen distance, for example, would be 2.90 Å which is smaller than the sum of their van der Waals radii (approximately 3.1 Å). Such a situation would lead to a hugely overestimated bending of the molecules and, thus, to an unphysical situation. To the best of our knowledge, the actual surface structure of F4TCNQ on Cu(111) has not yet been determined, and it is not even known whether a commensurate structure is formed at all.

C. Experimental methodology

Of primary interest was a photoemission study of F4TCNQ on Ag(111), as for this system experimental data are scarce.[29] The experiments presented in the present paper were performed at the FLIPPER II end-station at HASYLAB (Hamburg, Germany).[59] The interconnected sample preparation chambers (base pressure 4×10^{-10} mbar) and analysis chamber (base pressure 2×10^{-10} mbar) allowed sample transfer without breaking ultrahigh vacuum conditions. The Ag(111) single-crystal substrate was cleaned by repeated cycles of annealing (up to 550 °C) and Ar-ion sputtering. F4-TCNQ (Fluka) was evaporated using a resistively heated pinhole source, at an evaporation rate of ca. 1 Å/min. The film mass thickness was monitored with a quartz-crystal microbalance. For all thickness values reported hereafter, identical sticking coefficients of the molecules on the metal substrate and on the microbalance were assumed. While the former can be expected to be close to unity, the sticking coefficient on the microbalance surface was most likely smaller, as it was pre-covered with other organic molecules from other experiments. This results in an underestimation of the actual F4TCNQ layer mass thickness on the metal substrate. Moreover, no detailed information on the growth mode of F4TCNQ on Ag(111) is available, thus island-growth cannot be excluded, particularly for thicker films. Spectra were recorded with a double-pass cylindrical mirror analyzer with an energy resolution of 200 meV. The photon energy was 22 eV. The secondary electron cutoff (SECO) was measured with the sample biased at −3.00 V. The errors of all given values of binding energies and SECO positions are estimated to be ±0.05 eV.

III. RESULTS AND DISCUSSION

Prior to discussing the packing-density dependence of the electronic structure as well as how the choice of the substrate metal affects the interaction, the general scenario encountered for F4TCNQ adsorption is discussed for a densely packed layer on Ag(111).

A. Densely packed F4TCNQ on Ag(111): interface energetics

Similar to its precursor TCNQ,[60] in which all fluorine atoms are replaced by hydrogen atoms, F4TCNQ is known to adopt a fully planar and quinoidal structure in the gas phase or as a molecular crystal.[61] This situation changes dramatically upon adsorption on Ag(111): F4TCNQ adopts a bent geometry with the nitrogen atoms 1.23 Å closer to the top metal layer than the π backbone, which indicates a strong attractive interaction between the –CN substituents and the metal surface. The central ring is calculated to be 3.61 Å above the top Ag layer. An equivalent situation is encountered for adsorption on the Au(111) and Cu(111) surfaces; the latter has been confirmed by x-ray standing-wave experiments albeit with a somewhat smaller bending than in the calculations.[37] Moreover, a distortion of the molecular skeleton from a quinoidal toward an aromatic structure is observed. This aromatic stabilization can be identified when comparing the bond-length changes in Table I. The geometric distortions are comparable to those of reduced TCNQ (Ref. 62) and are a first indication for a charging of the molecule.

TABLE I. Bond lengths in isolated F4TCNQ molecules and in F4TCNQ adsorbed in a densely packed layer on Ag(111). The numbering of the bonds listed in the second column is shown in Fig. 1(c). The last column contains the bond-length changes.

Bond	Nb	$r_{\text{isolated F4TCNQ}}$/Å	$r_{\text{adsorbed F4TCNQ}}$/Å	Δr/Å
$N\equiv C$	1	1.19	1.20	+0.01
$C-C$	2	1.43	1.40	−0.03
$C=C$	3	1.40	1.46	+0.06
$C-C$	4	1.44	1.41	−0.03
$C=C$	5	1.37	1.39	+0.03

The particularly large electron affinity (EA) of F4TCNQ [3.68 eV for the vertical EA and 3.81 eV for the adiabatic EA (Ref. 63)] implies that such charge transfer should correspond to filling the lowest unoccupied molecular orbital (LUMO) of F4TCNQ, which in the noninteracting case would lie below the Fermi level of the metal. Indeed, a more or less complete filling of the LUMO with approximately two electrons has been suggested on the basis of UV photoelectron spectra (UPS).[27,29] The inconsistency in this picture is, however, that moving two electrons from the top metal layer by about 3 Å to the molecular π system would result in a dipole moment of 6 eÅ, 29 Debye(D), per molecule. According to the Helmholtz equation, this would result in a work-function increase by approximately 9 eV for a densely packed layer. This is not only unrealistically large and also inconsistent with the UPS data, but would also shift the energetic levels of F4TCNQ in a way that the (now filled) LUMO would come to lie significantly above the metal Fermi level—and, thus, should not be occupied at all. These considerations imply that the charge transfer between Ag and F4TCNQ as well as the resulting work-function modification are significantly more complex than expected and, therefore, deserve a more in-depth investigation.

The actual calculated electron potential energy for the Ag slab prior to (dashed line) and subsequent to F4TCNQ adsorption (solid line) is shown in the left part of Fig. 2. Upon adsorption, an increase in the electron potential energy is clearly visible on the F4TCNQ side of the slab (as indicated

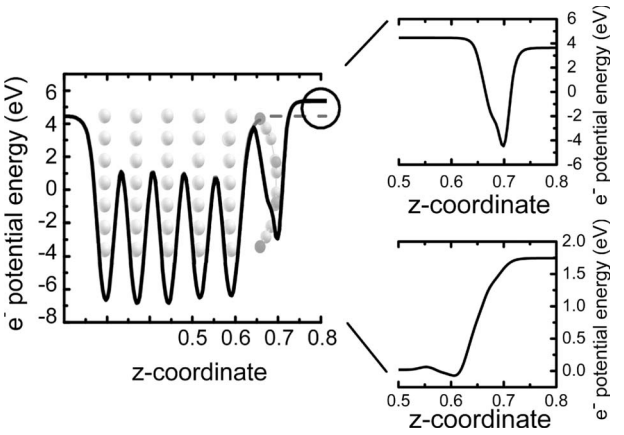

FIG. 2. Energetics of the adsorption of F4TCNQ on Ag(111) as a densely packed monolayer. Left: Plane averaged electron potential energy of the acceptor metal system in its final fully relaxed structure (solid line) and plane averaged potential energy of the metal slab alone (dashed line). The structure of the system is shown in the background as a guide to the eye. The two energies significantly differ only in the region where the acceptor molecule is adsorbed; in particular, the energy above the slab is shifted by the adsorbate. The circle highlights the work-function modification of upon adsorption of F4TCNQ. The latter results from a superposition of the effects plotted to the right. Right—Top: Plane averaged electron potential energy of the F4TCNQ monolayer in its final structure (but without the metal present). Right—Bottom: The effect of the charge rearrangements on the electron potential-energy landscape. The z range in the two right graphs is limited compared to the left plot to ease the comparison of all three figures.

by the circle). This corresponds to a work-function increase of +0.90 eV. In analogy to the situation for thiolate-bonded self-assembled monolayers the work-function modification can be partitioned into a "molecular" contribution, ΔE_{vac}, and a contribution due to the interfacial charge rearrangement [usually referred to as the bond dipole (BD)][22,64]

$$\Delta\phi = \mathrm{BD} + \Delta E_{\mathrm{vac}}. \tag{1}$$

"Molecular contribution" here means the possible impact of the molecular monolayer that is not associated with charge transfer from/to the metal. When adsorbing (di)polar molecules, it is related to the molecular dipole moment perpendicular to the surface. Such an (infinitely) extended dipole layer results in a shift of the vacuum level by

$$\Delta E_{\mathrm{vac}} = \frac{1}{\varepsilon_0 A}\mu. \tag{2}$$

μ refers to the dipole moment per molecule in the monolayer (including, e.g., depolarization effects),[65,66] ε_0 is the vacuum permittivity, and A is the area per molecule. In the present case, the situation is insofar less straightforward, as isolated F4TCNQ molecules do not possess any dipole moment (they are centrosymmetric). However, as discussed above, this changes due to adsorption. In the distorted conformation of the monolayer, each individual F4TCNQ molecule possesses a dipole moment of −2.69 D.[67] In effect it points away from the metal surface. ΔE_{vac} can, therefore, be regarded as the contribution to the work function change that results from the adsorption-induced geometric distortion of the F4TCNQ molecules. However, if it were the only constituent of $\Delta\Phi$, F4TCNQ adsorption would result in a work function *decrease* by −0.85 eV on Ag(111). This can also be seen in the top right part of Fig. 2, which shows the electron potential energy calculated for the F4TCNQ monolayer in the absence of the metal but in the geometry the molecules will adopt following adsorption.

In addition to the distortion, the interaction between Ag and F4TCNQ, however, results in significant interfacial charge rearrangements. They can be extracted from our calculations by subtracting the charge densities of the noninteracting systems, i.e., the Ag slab, $\rho_{\mathrm{Ag(111)}}$, and the monolayer, ρ_{mono},[68] from that of the combined system, ρ,

$$\Delta\rho_{\mathrm{bond}}(\vec{r}) = \rho(\vec{r}) - [\rho_{\mathrm{Ag(111)}}(\vec{r}) + \rho_{\mathrm{mono}}(\vec{r})]. \tag{3}$$

All charge densities are calculated self-consistently for the individual subsystems in the geometries they eventually adopt in the combined Ag/F4TCNQ system. As discussed above, the effects resulting from geometry changes in the monolayer are already accounted for in ΔE_{vac}. The resulting charge rearrangements then result in a modification of the potential-energy landscape for the electrons that can be derived from the Poisson equation

$$\nabla^2 E(\vec{r}) = \frac{e}{\varepsilon_0}\Delta\rho_{\mathrm{bond}}(\vec{r}). \tag{4}$$

The values integrated over the x-y plane, $E(z)$, are shown in the bottom right part of Fig. 2. In this way, the contribution of the interfacial charge rearrangements to the change in the system work function [corresponding to BD in Eq. (1)] is obtained; it amounts to +1.70 eV. Consequently, the charge rearrangements result in a pronounced *increase* in the work function, as expected for the adsorption of a strong acceptor like F4TCNQ. The net effect, i.e., the sum of ΔE_{vac} [Eq. (2)] and BD [see Eq. (1)], is a work-function *increase* by +0.85 eV. Hence, the geometric distortions upon adsorption compensate half of the charge-transfer effect. This implies that geometry changes have to be kept in mind when designing new acceptor materials for surface modifications. Still, both $\Delta\Phi$ with +0.85 eV, as well as BD with +1.70 eV, are significantly smaller than the values estimated from simple electrostatic considerations based on doubly occupying the molecular LUMO (vide supra). This makes it necessary to investigate the charge rearrangements at the interface in more detail.

B. Charge rearrangements at the interface

Contour plots of the charge rearrangements upon adsorption calculated using Eq. (3) are shown in Fig. 3 together with an isodensity representation of the LUMO orbital of the isolated molecule (to avoid confusions, the sign of the wave function is not considered in the latter case). In Figs. 3(a) and 3(b), electrons flow from the dark to the light gray areas. By comparing these charge rearrangements with the shape of the LUMO orbital of the isolated F4TCNQ molecule in Fig. 3(c), electron transfer into the LUMO can be unambiguously

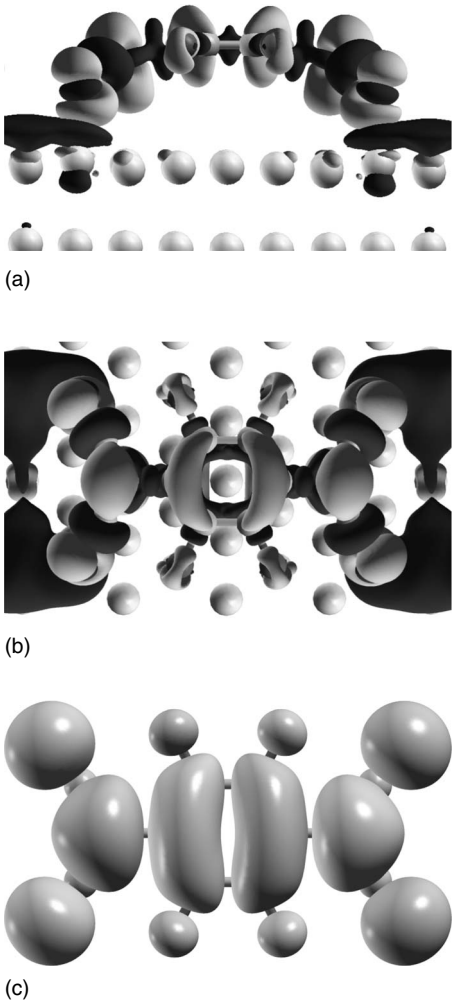

FIG. 3. From top to bottom: (a) Side and (b) top view of the three-dimensional charge-density rearrangements for F4TCNQ adsorption on Ag(111) (dense packing). Electrons flow from the dark gray to the light gray areas. In (a) only the top two metal rows are shown; in (b) only the top metal layer is shown. In (c) the molecular LUMO of F4TCNQ is displayed (note that the unlike usually done when plotting molecular orbitals, no difference in shading is used to denote the phase of the wave function to avoid confusions).

confirmed. The regions of electron accumulation are concentrated on those bonds that are shortened upon adsorption [cf. Table I and Fig. 1(a)]. The electron density on the metal is clearly decreased (dark area)—in particular, right underneath the –CN substituents of F4TCNQ. Moreover, there is also a pronounced electron depletion in the σ system in the –CN regions, whose origin will become clear when discussing changes in the orbital occupation of F4TCNQ upon adsorption.

Prior to that, the charge rearrangement integrated over the x-y plane within a unit cell, $\Delta\rho_{\mathrm{bond}}(z)$, needs to be discussed. It provides some additional insight into changes in the charge density and allows an easy comparison of charge rearrangements obtained at different packing densities or for different substrate metals (as discussed in later sections of this paper). First of all, $\Delta\rho_{\mathrm{bond}}(z)$ shown in the top part of Fig. 4 confirms the increased electron density in the π-electron region of

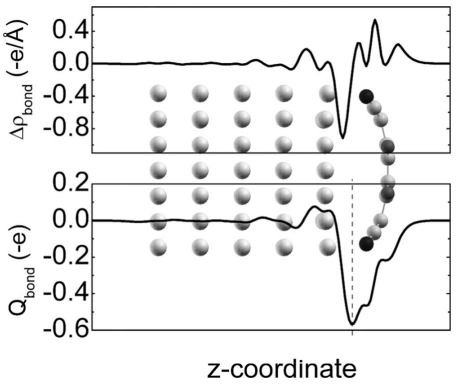

FIG. 4. Top: charge-density rearrangement, $\Delta\rho_{\mathrm{bond}}$, upon adsorption of a densely packed F4TCNQ monolayer on a Ag(111) surface integrated over the x-y plane within the unit cell; Bottom: resulting total charge transferred, Q_{bond}. The vertical line denotes the maximum value of Q_{bond} (for details see text). The structure of the combined system is shown in the background as a guide to the eye. Note that e corresponds to the (positive) elementary charge. Hence, with the unit of the y axis being $(-e/\text{Å})$, positive y values correspond to electron accumulation (i.e., charge depletion) and negative values to electron depletion (i.e., charge accumulation).

F4TCNQ as well as a pronounced electron depletion directly above the top metal layer. The charge rearrangements within the metal slab are confined to the immediate interface region; the electron density in the bottom three layers is virtually unaffected by the presence of the adsorbate. A "dip" in $\Delta\rho_{\mathrm{bond}}(z)$ in the region of the –CN substituents is also clearly resolved consistent with the decreased σ-electron density in that part of the molecule.

To assess the total amount of transferred charge, it is useful to integrate $\Delta\rho_{\mathrm{bond}}(z')$ over z' from below the slab to a certain position z. This gives the quantity $Q_{\mathrm{bond}}(z)$

$$Q_{\mathrm{bond}}(z) = \int_0^z \Delta\rho_{\mathrm{bond}}(z')dz', \tag{5}$$

which is shown in the bottom part of Fig. 4 for a F4TCNQ monolayer on Ag(111).

$Q_{\mathrm{bond}}(z)$ gives the charge shifted from the region below a plane at position z to the region above z. It steeply decreases above the metal plane (electron depletion), reaches a minimum (dashed line in Fig. 4), and then increases in the region of the molecule (electron accumulation) reaching zero above the molecular layer (as imposed by the condition of overall charge neutrality). It displays the clear signature of electron transfer from the metal to F4TCNQ. There is no unambiguous way to determine the actual amount of that transfer, as no clear distinction between the spatial region associated with the molecule and the metal is possible. Here, we define the maximum value of $Q_{\mathrm{bond}}(z)$ as the amount of transferred charge. For a monolayer of F4TCNQ it amounts to 0.56 electrons per molecule. In the following, we will compare that value to the charge transfer obtained from a more conventional (but usually more ambiguous) atomic-orbital-based partitioning scheme.

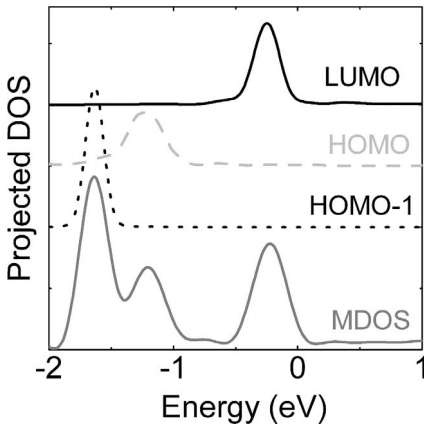

FIG. 5. Partitioning of the DOS of F4TCNQ on Ag(111) into contributions from individual molecular orbitals. From top to bottom: contribution of the molecular LUMO, the molecular HOMO, and the molecular HOMO-1; bottom: MDOS, i.e., the total molecular contribution. The Fermi is chosen as the origin of the energy axis.

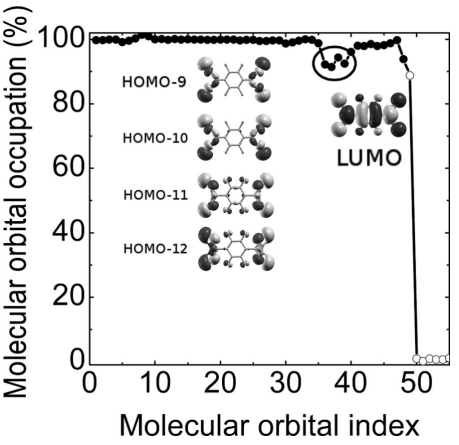

FIG. 6. Molecular orbital population analysis for F4TCNQ adsorbed on Ag(111) in a dense monolayer. The bands derived from the isolated molecular system were taken as reference for the projection. The full (open) circles correspond to molecular orbitals occupied (unoccupied) prior to adsorption. The reason for some occupation numbers to be above 100% is a well-known shortcoming of the adopted Mulliken population analysis.

Alternatively to analyzing the charge rearrangements due to bond formation in real space, one can describe them in a molecular-orbital picture. In this way, the question can be addressed which of the molecular orbitals loses or gains electrons as a result of the interaction with the metal. In this context, it is important to point out that such changes in orbital occupation can also be fractional. This is because upon contact with the metal, molecular and metal states hybridize and such hybrid bands can be partially occupied. This is especially expected for states close to the Fermi level. An elegant way to trace down such effects for the metal-organic interface is to project the DOS onto the molecular orbitals of the noninteracting adsorbate layer (i.e., the molecular layer with no metal present).[69–73] This allows assigning contributions to the total DOS to specific molecular orbitals. Here, we use the definition of the molecular-orbital projected DOS (MODOS) outlined in Ref. 73,

$$\mathrm{MODOS}_m(E) = \sum_{i,l,\vec{k}} c^{M^*}_{im\vec{k}} c^{M}_{il\vec{k}} \hat{S}_{ml\vec{k}} \delta(E - \varepsilon_{i\vec{k}}). \tag{6}$$

The $c^{M}_{im\vec{k}}$ are the linear combination of molecular-orbital (LCMO) coefficients and $\hat{S}_{ml\vec{k}}$ is the overlap matrix of the molecular orbitals (for further details see Ref. 73). The MODOS can, for instance, be used to determine how a particular MO is aligned with respect to the Fermi level even in the case of strong hybridization between metal and molecular states. This is shown for selected molecular orbitals in Fig. 5 for F4TCNQ on Ag(111). The molecular part to the total DOS (MDOS) of the system is shown in the bottom curve. In the displayed energy range, it can be partitioned into contributions from the LUMO, the highest occupied molecular orbital (HOMO), and the HOMO-1. One observes that the molecular LUMO is clearly responsible for the peak in the DOS just below the Fermi edge. The broadening of the respective MODOS features is a measure for the hybridization of the corresponding molecular state with metal orbitals (on top of the "external" broadening here set to 0.1 eV when plotting the DOS).

By integrating the MODOS associated with a particular molecular orbital, m, up to the Fermi energy, one can obtain a nominal occupation, O_m, of that orbital

$$O_m = \int_{-\infty}^{E_F} \mathrm{MODOS}_m(E) dE. \tag{7}$$

This then allows analyzing the bonding-induced charge transfer for each individual orbital, as shown in Fig. 6 for the densely packed F4TCNQ monolayer on Ag(111).

One can clearly see that—as a consequence of the interfacial charge transfer—the LUMO is almost completely filled (filling of 89%, i.e., by approximately 1.8 electrons). This is in agreement with the conclusions drawn before from the real-space charge-transfer picture in Fig. 3. At the same time, however, four deeper lying orbitals (HOMO-9–HOMO-12) have significantly lost electrons. They can be identified as σ orbitals largely localized on the –CN groups. These orbitals strongly participate in the bonding of the F4TCNQ molecule to the substrate, as can also be inferred from the bending of the molecule. The reason why nominally deep lying rather than frontier orbitals are responsible for that σ-electron transfer lies in their particularly strong hybridization with the metal states.[37] In some sense, one could thus consider the –CN groups as docking groups, strongly linking the F4TCNQ layer to the Ag substrate.

This situation of charge forward and backward donation involving σ and π orbitals is reminiscent of the Blyholder model[74] applied, e.g., to the bonding of CO on various metals, such as Pt(111),[75,76] Cu(111),[76] Ag(111),[76] Au(111),[76] Al(111),[77] and Fe(100).[78]

C. Dependence of the electronic structure on the packing density

As a next step, we analyze how the packing density of the F4TCNQ layer influences the electronic properties of the Ag/

TABLE II. Area of the unit cell, work-function modification $\Delta\Phi$, distortion induced change in the electrostatic energy, ΔE_{vac}, bond dipole (BD), "total" transferred charge, Q_{bond}, and binding energy, E_{bind}. The values for $\Delta\Phi$, ΔE_{vac}, and BD are given in eV as well as in Debye, where the former refers to the actual energy and latter denotes the corresponding unit-cell dipole moment. All quantities are listed for F4TCNQ on Ag(111) and Au(111) in monolayer as well as submonolayer coverage (cf. Fig. 1); for adsorption on Cu(111) only the values for submonolayer coverage have been calculated (cf. Sec. II). The ratios of all values for different coverages are also given.

Metal	Area (Å^2)	$\Delta\Phi$ (eV)/(D)	ΔE_{vac} (eV)/(D)	BD (eV)/(D)	Q_{bond} (e)	E_{bind} (eV)
Ag_{ML}	115	0.85/2.59	−0.85/−2.59	1.70/5.19	0.56	2.10
Ag_{subML}	225	0.51/3.05	−0.47/−2.81	0.98/5.85	0.55	1.90
Ratio	1.95	1.67/0.85	1.81/0.92	1.73/0.89	1.02	1.11
Au_{ML}	116	0.29/0.93	−0.79/−2.55	1.07/3.46	0.34	0.90
Au_{subML}	226	0.33/1.98	−0.33/−1.98	0.66/4.01	0.38	0.75
Ratio	1.94	0.88/0.47	2.39/1.29	1.62/0.86	0.89	1.20
Cu_{subML}	172	0.19/1.13	−0.82/−4.88	1.01/6.00	0.44	2.70

F4TCNQ interface. This is insofar interesting as, experimentally, a strong linear dependence of the F4TCNQ induced work-function modification on the nominal coverage has been observed.[26,29] On the other hand, a pronounced nonlinear evolution with coverage has been discussed for $\Delta\Phi$ and the level alignment for the adsorption of 4′-substituted 4-mercaptobiphenyls on Au(111).[65] Moreover, submonolayers of organic molecules on metals are interesting as they allow addressing the limiting case of isolated molecules on metals, an aspect of particular interest in the emerging field of molecular electronics.

Here, the effect of coverage is addressed by comparing the work-function modifications as well as its two contributions, BD and ΔE_{vac}, for the two unit cells shown in Figs. 1(b) and 1(c). Each unit cell contains one F4TCNQ molecule. The unit cell for the loosely packed layer is nearly twice as big as in the densely packed case. $\Delta\Phi$, ΔE_{vac}, and BD for the two packing densities are listed in Table II. In addition to reporting the energies in eV, also the respective contributions to the z components of the dipole moments per unit cell are given in Debye (D). The latter are useful, as they are independent of the unit-cell size, and, therefore, ideal for addressing depolarization effects. The other values listed in Table II are the total transferred charge, Q_ρ, and the binding energy (BE), E_{bind}, per molecule.[79]

As far as the work-function modifications are concerned, one observes a slightly sublinear increase with increasing the coverage (i.e., while the packing increases by a factor of 1.95, the work function increases by a factor of only 1.67). This also manifests itself in the dipole moment of the unit cell, which is 3.05 D in the submonolayer coverage and is decreased to 2.59 D (i.e., by 15%) for the monolayer coverage. This is a possible indication of depolarization effects in the densely packed layer; i.e., the neighboring bonding-induced dipoles reduce each other. Overall, this effect is relatively weak. To determine its origin, it is useful to first analyze the evolutions of ΔE_{vac} and BD separately.

ΔE_{vac} changes only slightly (the ratio of the corresponding dipoles is computed to be 0.92). The reason for that lies in the almost identical geometrical structures in the monolayer and submonolayer cases on Ag(111). The nitrogen atoms of F4TCNQ are located about 2.38 Å above the top metal surface in the monolayer setup. In the submonolayer case, they are located 2.39 Å above the metal surface. The central ring is located 1.19 Å above the nitrogen atoms in the former case and 1.20 Å in the latter case. Hence, the vertical adsorption distance and the bent are hardly affected by increasing the packing density.

BD, on the other hand, experiences slightly larger depolarization effects. The associated dipole moment decreases from 5.85 D to 5.19 D (i.e., by 11%) when going from submonolayer to monolayer coverage. Considering the origin of BD, this has to be a consequence of the adsorption-induced charge rearrangements, $\Delta\rho_{bond}$. The total charge transferred, i.e., the maximum of Q_{bond}, is nearly the same for both packing densities; the shape of $\Delta\rho_{bond}$, however, differs. Compared to the charge rearrangements shown for the densely packed case in Fig. 4, at reduced coverage the electron accumulation is somewhat more pronounced in the area above the plane of the central ring and correspondingly reduced below the π plane (plot not shown). As far as changes in the orbital population are concerned, the MODOS derived occupation of the LUMO is increased by about 10% in the submonolayer case. This is consistent with a shift of the LUMO associated peak away from the metal Fermi level by 0.2 eV as shown in Fig. 7.

A possible explanation for the relatively weak depolarization effects lies in the peculiar dipole distribution that arises due to the superposition of forward and backward donation processes. While the electron density is increased in the π backbone, it is decreased on parts of the –CN groups (compare Figs. 3 and 4). A simplified schematic representation of the resulting dipole structure is shown in Fig. 8. A dipole pointing toward the metal surface can be associated locally with the –CN groups (σ dipole). Another one pointing away from the metal will be delocalized over the whole π system (π dipole). At dense packing, the molecular rows are displaced with respect to each other on the surface. Therefore, the σ dipoles pointing downwards in one row will come to lie close to the π dipoles pointing upwards in the neighbor-

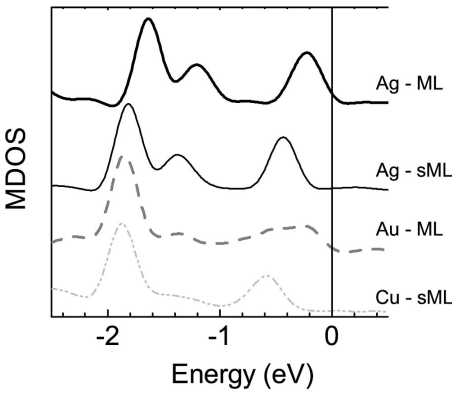

FIG. 7. Calculated MDOS for F4TCNQ adsorbed on Ag(111) in the monolayer and submonolayer regimes, as well as for F4TCNQ on Au(111) at monolayer coverage and for a submonolayer F4TCNQ on Cu(111). The corresponding structures are chosen according to Fig. 1. The Fermi energy was chosen as the origin of the energy axis.

ing row. Therefore, the mutual depolarization of the π dipoles is to some extent compensated by a dipole enhancement due to the interaction with the closer lying (albeit weaker) σ dipoles.

What remains to be explained is why the biggest deviation from linear coverage dependence is observed for the work-function modification: The reason for that is that $\Delta\Phi$ is obtained by subtracting ΔE_{vac} from the approximately twice as big BD. As the dipole moment associated with ΔE_{vac} remains nearly the same, an only slightly changing value is subtracted from the more strongly changing dipole associated with BD. Consequently, the relative changes in $\Delta\Phi$ are the strongest of all involved quantities.

D. Impact of the substrate metal

When comparing the role of different coinage metals as substrates, one has to distinguish between the low and high-coverage case. The latter is accessible only for Au and Ag (see Sec. II B). The former is accessible for all coinage metals used in the present contribution including Cu(111). The (111) surfaces of those metals are characterized by significantly different work functions. We calculated values of 5.25 eV for Au(111) and 4.49 eV for Ag (111), which are in excellent agreement with our measurements [5.3 eV (Ref. 26) for pristine Au(111) and 4.5 eV for Ag(111), this work]. The work function of Cu(111) is intermediate between Ag and Au and is calculated (measured) to be Φ=4.82 eV (4.9 eV) (Ref. 80) for pristine Cu(111).

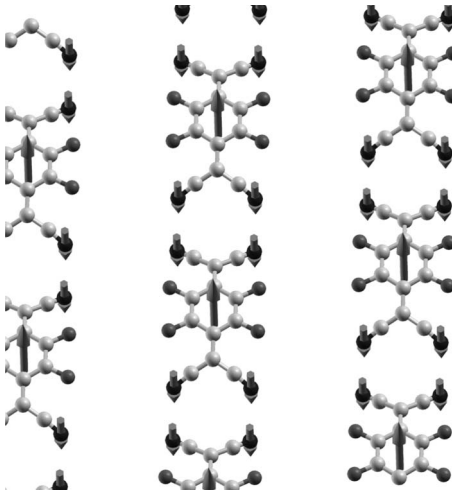

FIG. 8. Dipole structure arising due to charge-transfer between F4TCNQ on Ag(111) at monolayer coverage. The metal atoms are not shown. The molecular rows are shifted relative to each other as observed experimentally.

The work-function modification, $\Delta\Phi$, differs quite significantly for Ag and Au in the high-coverage regime and is distinctly bigger for Ag(111). The values are +0.85 eV for Ag and +0.29 eV for Au. This leads to both F4TNQ covered metals ending up with virtually identical work functions (5.54 eV for Au; 5.34 eV for Ag). Such a trend is also observed both experimentally as well as theoretically for self-assembled thiolate monolayers on the same metals.[21,73,81] This means that F4TCNQ exhibits a much greater influence on Ag, which again has to be related either to the monolayer contribution, ΔE_{vac}, and/or differences in BD resulting from different interfacial charge rearrangements. From the corresponding values in Table II, one can conclude that the monolayer contribution is, in fact, not responsible for the observed difference, as both ΔE_{vac} contributions differ only slightly (−0.85 eV for Ag and −0.79 eV for Au). This is again a consequence of very similar adsorption geometries: The nitrogen atoms are located 2.44 Å (Au) and 2.38 Å (Ag) above the metal, and also the adsorption distances of the central carbon atoms are very similar [1.23 Å (Au) and 1.19 Å (Ag) above the nitrogen atoms]. The charge rearrangements, however, differ to a much greater extent. The total charge transferred, Q_{bond}, is by more than 60% larger on Ag (111) (0.56 electrons on Ag versus 0.34 electrons on Au). As the arrangement of the molecules on the surface is assumed to be identical in both cases (see above), considerations regarding dipole arrangements as discussed before for the packing-density dependence do not apply here.

Instead, as shown in Fig. 9, we find that more electron density is depleted between the top metal atoms and the plane of the nitrogen atoms in the Ag case. The extra electrons are, however, not shifted toward the top Ag layer, where they would give rise to an extra bond dipole that would decrease the metal work function. On the contrary, less electron density is accumulated in the top metal layer than in the Au(111) case. Instead, the electrons from the interfacial region of Ag/F4TCNQ are to a distinctly larger extent transferred onto the F4TCNQ acceptor layer than it is the case of the Au/F4TCNQ system.

Interestingly, the difference between the work functions of the pristine substrates is compensated by the charge rearrangements also as far as the level alignments are concerned. Hence, the molecular LUMO-derived peaks are pinned at about 0.3 eV below the Fermi level in both cases (Fig. 7). Another indication for the stronger interaction of F4TCNQ with Ag(111) compared to Au(111) is the significantly larger binding energy in the former case (2.1 eV compared to 0.9 eV).[79]

The situation is somewhat different for adsorption on Cu(111), which for the reasons discussed in the methodology

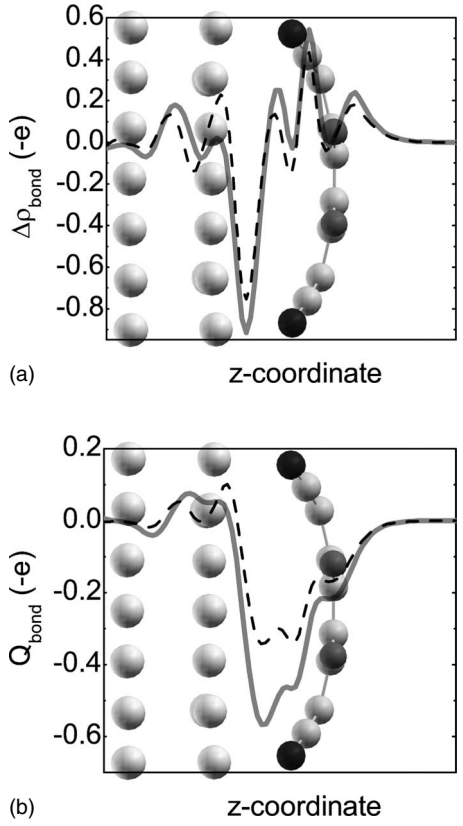

FIG. 9. (a) Comparison of charge rearrangements, $\Delta\rho_{\text{bond}}$, for densely packed layers of F4TCNQ adsorbed on Ag(111) (solid gray) and Au(111) (dashed black). (b) Comparison of the total transferred charges, Q_{bond}. The structure of the molecules on Ag(111) is shown in the background as a guide to the eye. Note that e corresponds to the (positive) elementary charge. Hence, with the unit of the y axis being ($-e$/Å), positive y values correspond to electron accumulation (i.e., charge depletion) and negative values to electron depletion (i.e., charge accumulation).

section could only be studied in the low coverage regime.[82] The monolayer contribution, ΔE_{vac}, on Cu(111) distinctively differs from the two other metals. In fact, it is almost twice as big in the Cu case (−0.82 eV) as in the corresponding Ag case (−0.47 eV). This is the consequence of a stronger bend of the molecule on Cu(111). In this context it, however, needs to be mentioned that a comparison between DFT-based calculations and x-ray standing-wave (XSW) experiments[37] indicates that the bent of F4TCNQ on Cu(111) is somewhat overestimated by the calculations. To what extent this is a general shortcoming of local DFT functionals due to their inability to describe van der Waals interactions or a problem related to the description of the Cu surface cannot be clearly decided at the moment, as, to the best of our knowledge, no XSW data for F4TCNQ adsorbed on other coinage metals are available. The BD associated with the F4TCNQ submonolayer on Cu(111) is virtually the same as on Ag(111) (1.01 eV in the Cu case and 0.98 eV for Ag), indicating that a similar amount of charge is transferred.

As far as the F4TCNQ submonolayer on Au is concerned, the expected picture evolves for the charge transfer, i.e., the total transferred charge is very similar to the densely packed situation and the dipole moment of the unit cell hardly changes with coverage. The values of BD increase close to linearly with the packing density. The adsorption geometry, however, significantly differs from all other investigated cases: The bending is strongly reduced and, thus, ΔE_{vac} decreases with the net effect of $\Delta\Phi$ being slightly larger in the submonolayer than in the monolayer case. This behavior is quite unexpected and its origin is not fully understood. Bearing in mind that the calculated binding energy is very low, it also cannot be entirely excluded, that it is at least in part a consequence of the applied methodology that, for example, does not take into account van der Waals interactions.[83]

E. Comparison between the theoretical predictions and experimental data

In this section physical observables derived from calculations, such as the adsorption-induced work-function modifications, $\Delta\Phi$, and the energetic positions of the molecular levels, will be compared to experimental UPS data. We will primarily focus on F4TCNQ on Ag(111) and present experimental data. Experimental data for F4TCNQ on (albeit polycrystalline) Au are taken from Ref. 26. For the case of F4TCNQ on Cu(111), a detailed comparison between theory and experiments can be found in Ref. 37.

Figure 10(a) contains valence-region UPS spectra of pristine Ag(111) and subsequently deposited F4TCNQ for nominal coverages up to 0.6 Å. Upon F4TCNQ adsorption, a distinctive feature appears in the lowest coverage spectrum at 1.15 eV BE at a coverage of 0.03 Å. In analogy to the situation on Au (Ref. 26) and Cu,[37] it can be identified as the formerly unoccupied LUMO of the neutral molecule, which has been filled as a result of the interfacial charge transfer and thus lies now clearly below E_F. With subsequent deposition of F4-TCNQ the LUMO-derived peak shifts toward lower BE, reaching a final position of 1.00 eV at 0.3 Å. This is in good agreement with the theoretical results presented above, where a shift of the LUMO-derived feature of 0.20 eV toward lower BE was predicted at submonolayer coverages (Sec. III C). The features at higher BE can be associated with the HOMO and HOMO-1 derived peaks from Fig. 5 (using the nomenclature appropriate for the neutral molecule). The HOMO-derived peak exhibits the same shift as that derived from LUMO and reaches a final position at 2.15 eV BE. Qualitatively, the agreement between the calculated density of states and the measured UPS spectra is reasonably good; the spacing between the peaks is, however, clearly larger in the experiments.[84] This is not unexpected bearing in mind that gradient-corrected functionals typically yield a too small spacing between molecular orbitals. This can, e.g., be inferred from comparing Kohn-Sham eigenvalues with quasiparticle excitation energies.[85–87] It is, therefore, common practice to expand the calculated spectra by multiplying them with a constant factor.[88,89] Furthermore, variations in the experimental spectra are observed when recording them at different angles,[90–92] an effect that is not accounted for in the presented calculations, in which UPS cross sections are not considered. Moreover, especially at submonolayer coverage the actual film-structure is not known and in the actually

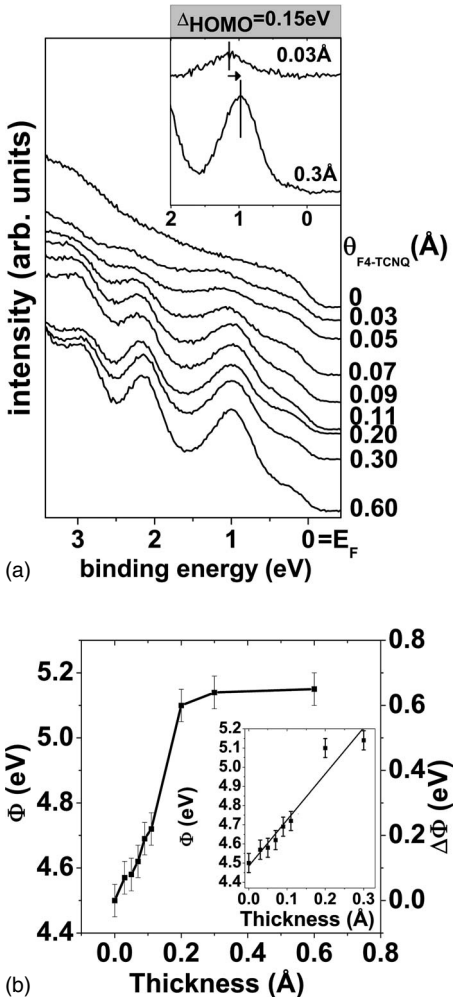

FIG. 10. (a) Near Fermi energy region UPS spectra of pristine Ag(111) and after sequential deposition of F4TCNQ. Photoemission features induced by F4TCNQ are clearly visible are at ca. 1.0 and 2.2 eV binding energy. Monolayer coverage is expected to occur at a nominal coverage of ca. 0.3 to 0.6 Å. The inset shows the LUMO-derived peak for 0.03 and 0.3 Å coverage after subtraction of appropriately weighted pristine Ag(111) spectra. (b) Work function Φ and work-function modification (ΔΦ) upon adsorption of F4TCNQ on Ag(111). The inset shows the submonolayer regime in more detail. The line is a linear fit to the data points from 0.03 to 0.3 Å coverage.

investigated samples deviations from the assumed ideal structure might play a prominent role.

As shown in Fig. 10(b), the sample work function Φ increases almost linearly with coverage from 4.5 eV [pristine Ag(111)] to about 5.15 eV at a nominal coverage of 0.3 Å [see inset in Fig. 10(b)]. At higher coverages, the work function remains virtually constant. Based on this finding, a nominal coverage of around 0.3 to 0.6 Å can be associated with almost full monolayer coverage. The measured maximum work function increase of about 0.65 eV for F4TCNQ on Ag(111) agrees very well with the calculated ΔΦ value of 0.85 eV for the densely packed monolayer, especially considering that the calculations assume a completely covered and perfectly ordered layer.

As far as the linear coverage dependence is concerned, two scenarios can be envisioned: One would be a gradual decrease in the average spacing between the adsorbate molecules with increasing coverage in analogy to the observation for tetrathiofulvalene (TTF) on Au(111).[38] There the structure arises from mutual electrostatic repulsion of the adsorbate molecules, which are charged as a result of the molecule to metal electron transfer. In that case, a close to linear increase in ΔΦ with the F4TCNQ surface density can be rationalized on the basis of the results of Sec. III C. Alternatively, also the formation of (small) F4TCNQ clusters, whose size and/or density increases with coverage, would result in a close to linear work-function increase.

A linear evolution of ΔΦ with coverage has also been observed on (polycrystalline) Au.[26] With ΔΦ=0.35 eV, the net effect is, however, much smaller than on Ag, again in excellent agreement with the calculations, which predict a work-function increase of only 0.29 eV for a densely packed F4TCNQ layer on Au(111) (cf. Table II).

IV. SUMMARY AND CONCLUSIONS

The present contribution provides a comprehensive theoretical description of the adsorption of the prototypical strong acceptor F4TCNQ on coinage metals. Such systems are particularly interesting as electrodes in organic (opto)electronic devices, as their work functions can be continuously tuned over a wide range. We find that the work-function increase due to the F4TCNQ layer originates from a subtle interplay between a molecular dipole resulting from bonding-induced distortions of the adsorbate and a bond dipole stemming from the interfacial charge transfer. The latter is a superposition of electron transfer from the metal into the π^* LUMO and back-transfer from σ states localized on the –CN substituents. This can be inferred, on the one hand, from an analysis of the real-space charge rearrangements and, on the other hand, from a projection of the molecular density of states onto the bands derived from the individual molecular orbitals.

Comparing the electronic structure of a system with full- and ca. half-monolayer packing on Ag(111), it is found that depolarization effects play only a minor role in the investigated system. A possible explanation for that is the peculiar arrangement of opposing dipoles as a result of the monolayer structure. Furthermore, weak depolarization is fully consistent with the experimentally observed linear dependence of the metal work function on F4TCNQ coverage.

Another interesting observation is that when covered by a densely packed F4TCNQ monolayer, the work functions of Au(111) and Ag(111) become similar despite the fact that the pristine work function of a pristine Au(111) surface is by ca. 0.7–0.8 eV larger than that of a Ag(111) surface. This is found to be primarily a consequence of the much larger net electron transfer from Ag to F4TCNQ.

The results of the calculations agree well with experimental data on Ag(111) and also previously published experimental results. This supports the validity of the developed detailed microscopic model for the electronic properties of the interfaces that is otherwise largely based on the quantum-mechanical modeling.

ACKNOWLEDGMENTS

The authors would like to acknowledge the financial support by the European Commission project "IControl" (Grant No. EC-STREP-033197). G.H. is supported by the Marie-Curie program under the INSANE project (OIF Contract No. 021511). The authors would also like to thank A. M. Track and F. Rissner for stimulating discussions and are grateful to the section "Computing & Application Services" of the Zentrale Informatikdienst of the Graz University of Technology for providing computational resources and to the Institut für Materialphysik of the Universität Wien for providing the VASP code.

[1] H. Ishii, K. Sugiyama, D. Yoshimura, E. Ito, Y. Ouchi, and K. Seki, IEEE J. Sel. Top. Quantum Electron. **4**, 24 (1998).
[2] H. Ishii, K. Sugiyama, E. Ito, and K. Seki, Adv. Mater. (Weinheim, Ger.) **11**, 605 (1999).
[3] H. Ishii, H. Oji, E. Ito, N. Hayashi, D. Yoshimura, and K. Seki, J. Lumin. **87-89**, 61 (2000).
[4] X. Crispin, V. Geskin, A. Crispin, J. Cornil, R. Lazzaroni, W. R. Salaneck, and J. L. Bredas, J. Am. Chem. Soc. **124**, 8131 (2002).
[5] A. Kahn, N. Koch, and W. Y. Gao, J. Polym. Sci., Part B: Polym. Phys. **41**, 2529 (2003).
[6] D. Cahen and A. Kahn, Adv. Mater. (Weinheim, Ger.) **15**, 271 (2003).
[7] N. Koch, J. Phys.: Condens. Matter **20**, 184008 (2008).
[8] H. Sirringhaus, N. Tessler, and R. H. Friend, Science **280**, 1741 (1998).
[9] R. H. Friend, R. W. Gymer, A. B. Holmes, J. H. Burroughes, R. N. Marks, C. Taliani, D. D. C. Bradley, D. A. D. Santos, J. L. Bredas, M. Logdlund, and W. R. Salaneck, Nature (London) **397**, 121 (1999).
[10] A. Crispin, X. Crispin, M. Fahlman, M. Berggren, and W. R. Salaneck, Appl. Phys. Lett. **89**, 213503 (2006).
[11] C. Tengstedt, W. Osikowicz, W. R. Salaneck, I. D. Parker, C.-H. Hsu, and M. Fahlman, Appl. Phys. Lett. **88**, 053502 (2006).
[12] N. Koch, ChemPhysChem **8**, 1438 (2007).
[13] L. Lindell, M. Unge, W. Osikowicz, S. Stafstrom, W. R. Salaneck, X. Crispin, and M. P. de Jong, Appl. Phys. Lett. **92**, 163302 (2008).
[14] I. H. Campbell, J. D. Kress, R. L. Martin, D. L. Smith, N. N. Barashkov, and J. P. Ferraris, Appl. Phys. Lett. **71**, 3528 (1997).
[15] R. W. Zehner, B. F. Parsons, R. P. Hsung, and L. R. Sita, Langmuir **15**, 1121 (1999).
[16] J. Morgado, A. Charas, and N. Barbagallo, Appl. Phys. Lett. **81**, 933 (2002).
[17] E. L. Bruner, N. Koch, A. R. Span, S. L. Bernasek, A. Kahn, and J. Schwartz, J. Am. Chem. Soc. **124**, 3192 (2002).
[18] H. Yan, Q. L. Huang, J. Cui, J. G. C. Veinot, M. M. Kern, and T. J. Marks, Adv. Mater. (Weinheim, Ger.) **15**, 835 (2003).
[19] C. Bock, D. V. Pham, U. Kunze, D. Kafer, G. Witte, and C. Woll, J. Appl. Phys. **100**, 114517 (2006).
[20] K. Asadi, F. Gholamrezaie, E. Smits, P. W. M. Blom, and B. de Boer, J. Mater. Chem. **17**, 1947 (2007).
[21] G. Heimel, L. Romaner, E. Zojer, and J. L. Bredas, Nano Lett. **7**, 932 (2007).
[22] G. Heimel, L. Romaner, E. Zojer, and J.-L. Bredas, Acc. Chem. Res. **41**, 721 (2008).
[23] M. Pfeiffer, A. Beyer, T. Fritz, and K. Leo, Appl. Phys. Lett. **73**, 3202 (1998).
[24] M. Pfeiffer, K. Leo, X. Zhou, J. S. Huang, M. Hofmann, A. Werner, and J. Blochwitz-Nimoth, Org. Electron. **4**, 89 (2003).
[25] W. Y. Gao and A. Kahn, J. Appl. Phys. **94**, 359 (2003).
[26] N. Koch, S. Duhm, J. P. Rabe, A. Vollmer, and R. L. Johnson, Phys. Rev. Lett. **95**, 237601 (2005).
[27] N. Koch, S. Duhm, J. P. Rabe, S. Rentenberger, R. L. Johnson, J. Klankermayer, and F. Schreiber, Appl. Phys. Lett. **87**, 101905 (2005).
[28] S. Duhm, H. Glowatzki, V. Cimpeanu, J. Klankermayer, J. P. Rabe, R. L. Johnson, and N. Koch, J. Phys. Chem. B **110**, 21069 (2006).
[29] S. Duhm, H. Glowatzki, J. P. Rabe, N. Koch, and R. L. Johnson, Appl. Phys. Lett. **90**, 122113 (2007).
[30] A. G. Werner, F. Li, K. Harada, M. Pfeiffer, T. Fritz, and K. Leo, Appl. Phys. Lett. **82**, 4495 (2003).
[31] C. K. Chan, E. G. Kim, J. L. Brédas, and A. Kahn, Adv. Funct. Mater. **16**, 831 (2006).
[32] E. Umbach, Prog. Surf. Sci. **35**, 113 (1990).
[33] A. Hauschild, K. Karki, B. C. C. Cowie, M. Rohlfing, F. S. Tautz, and M. Sokolowski, Phys. Rev. Lett. **94**, 036106 (2005).
[34] N. Koch, G. Heimel, J. Wu, E. Zojer, R. L. Johnson, J.-L. Brédas, K. Müllen, and J. P. Rabe, Chem. Phys. Lett. **413**, 390 (2005).
[35] Y. Zou, L. Kilian, A. Scholl, T. Schmidt, R. Fink, and E. Umbach, Surf. Sci. **600**, 1240 (2006).
[36] F. S. Tautz, Prog. Surf. Sci. **82**, 479 (2007).
[37] L. Romaner, G. Heimel, J.-L. Bredas, A. Gerlach, F. Schreiber, R. L. Johnson, J. Zegenhagen, S. Duhm, N. Koch, and E. Zojer, Phys. Rev. Lett. **99**, 256801 (2007).
[38] I. Fernandez-Torrente, S. Monturet, K. J. Franke, J. Fraxedas, N. Lorente, and J. I. Pascual, Phys. Rev. Lett. **99**, 176103 (2007).
[39] C. Huckstadt, S. Schmidt, S. Hufner, F. Forster, F. Reinert, and M. Springborg, Phys. Rev. B **73**, 075409 (2006).
[40] E. Ito, H. Oji, H. Ishii, K. Oichi, Y. Ouchi, and K. Seki, Chem. Phys. Lett. **287**, 137 (1998).
[41] G. Kresse and J. Furthmuller, Phys. Rev. B **54**, 11169 (1996).
[42] G. Kresse and J. Furthmuller, Comput. Mater. Sci. **6**, 15 (1996).
[43] P. E. Blöchl, Phys. Rev. B **50**, 17953 (1994).
[44] G. Kresse and D. Joubert, Phys. Rev. B **59**, 1758 (1999).
[45] H. J. Monkhorst and J. D. Pack, Phys. Rev. B **13**, 5188 (1976).
[46] M. Methfessel and A. T. Paxton, Phys. Rev. B **40**, 3616 (1989).
[47] J. M. Soler, E. Artacho, J. D. Gale, A. Garcia, J. Junquera, P. Ordejon, and D. Sanchez-Portal, J. Phys.: Condens. Matter **14**, 2745 (2002).
[48] L. Romaner, G. Heimel, M. Gruber, J. L. Bredas, and E. Zojer, Small **2**, 1468 (2006).
[49] L. Romaner (unpublished).
[50] A. Kokalj, Comput. Mater. Sci. **28**, 155 (2003).
[51] M. J. Frisch *et al.*, GAUSSIAN03 (Gaussian, Inc., Pittsburgh, PA, 1998).

[52] R. Krishnan, J. S. Binkley, R. Seeger, and J. A. Pople, J. Chem. Phys. **72**, 650 (1980).
[53] P. M. W. Gill, B. G. Johnson, J. A. Pople, and M. J. Frisch, Chem. Phys. Lett. **197**, 499 (1992).
[54] A. D. Becke, J. Chem. Phys. **98**, 5648 (1993).
[55] C. Lee, W. Yang, and R. G. Parr, Phys. Rev. B **37**, 785 (1988).
[56] S. R. Marder, B. Kippelen, A. K. Y. Jen, and N. Peyghambarian, Nature (London) **388**, 845 (1997).
[57] F. Jackel, U. G. E. Perera, V. Iancu, K. F. Braun, N. Koch, J. P. Rabe, and S. W. Hla, Phys. Rev. Lett. **100**, 126102 (2008).
[58] The $\langle 11-2 \rangle$ direction was fully optimized and single-point calculations on the rotated atoms where performed for the other setups. Moreover comparisons of different fully optimized setups on Cu(111) and Au(111) did not show differences.
[59] R. L. Johnson and J. Reichardt, Nucl. Instrum. Methods Phys. Res. **208**, 791 (1983).
[60] R. E. Long, R. A. Sparks, and K. N. Trueblood, Acta Crystallogr. **18**, 932 (1965).
[61] T. J. Emge, M. Maxfield, D. O. Cowan, and T. J. Kistenmacher, Mol. Cryst. Liq. Cryst. **65**, 161 (1981).
[62] M. S. Khatkale and J. P. Devlin, J. Chem. Phys. **70**, 1851 (1979).
[63] Both EA values were obtained using GAUSSIAN03 at the 6-31G(d,p) level. The adiabatic EA allows the structure in the excited level to relax whereas the vertical EA does not take this into account.
[64] G. Heimel, L. Romaner, J. L. Bredas, and E. Zojer, Phys. Rev. Lett. **96**, 196806 (2006).
[65] L. Romaner, G. Heimel, and E. Zojer, Phys. Rev. B **77**, 045113 (2008).
[66] D. Cornil, Y. Olivier, V. Geskin, and J. Cornil, Adv. Funct. Mater. **17**, 1143 (2007).
[67] This value is obtained for calculations of the monolayer in its final geometry in the absence of the metal substrate.
[68] Here, the slab and the monolayer are considered both in their final geometries that they will assume in the combined system; this is necessary, as the impact of the adsorption-induced geometric distortions has already been accounted for by ΔE_{vac}.
[69] T. Hughbanks and R. Hoffman, J. Am. Chem. Soc. **105**, 1150 (1983).
[70] R. Hoffmann, Rev. Mod. Phys. **60**, 601 (1988).
[71] C. J. Nelin, P. S. Bagus, and M. R. Philpott, J. Chem. Phys. **87**, 2170 (1987).
[72] I. H. Campbell, S. Rubin, T. A. Zawodzinski, J. D. Kress, R. L. Martin, D. L. Smith, N. N. Barashkov, and J. P. Ferraris, Phys. Rev. B **54**, R14321 (1996).
[73] G. M. Rangger, L. Romaner, G. Heimel, and E. Zojer, Surf. Interface Anal. **40**, 371 (2008).
[74] G. Blyholder, J. Phys. Chem. **68**, 2772 (1964).
[75] H. Aizawa and S. Tsuneyuki, Surf. Sci. **399**, L364 (1998).
[76] B. Hammer, Y. Morikawa, and J. K. Nørskov, Phys. Rev. Lett. **76**, 2141 (1996).
[77] T. C. Chiang, G. Kaindl, and D. E. Eastman, Solid State Commun. **36**, 25 (1980).
[78] G. Blyholder and M. Lawless, Surf. Sci. **290**, 155 (1993).
[79] Here, the binding energy is calculated via subtraction of the metal slab energy and the F4TCNQ monolayer energy from the system energy in the same unit cells.
[80] S. Duhm, A. Gerlach, I. Salzmann, B. Bröker, R. L. Johnson, F. Schreiber, and N. Koch, Org. Electron. **9**, 111 (2008).
[81] C. D. Zangmeister, L. B. Picraux, R. D. van Zee, Y. Yao, and J. M. Tour, Chem. Phys. Lett. **442**, 390 (2007).
[82] Small numerical deviations compared to the numbers reported in Ref. 37 are due to the fact that here we described the substrate by five metal layers, compared to four layers in our previous study. This slightly changes the numbers but affects the qualitative conclusions in no way.
[83] Note that the here presented results stem from a local minimum in the energy, where the F4TCNQ is adsorbed flat, i.e., a slight perturbation results in a twist of the molecule along its long molecular axis which is an energetically favored configuration.
[84] Note that here especially the peak associated with the filled former LUMO is emerging too close to the Fermi energy in the calculation.
[85] S. Kümmel and L. Kronik, Rev. Mod. Phys. **80**, 3 (2008).
[86] M. S. Hybertsen and S. G. Louie, Phys. Rev. B **34**, 5390 (1986).
[87] R. O. Jones and O. Gunnarsson, Rev. Mod. Phys. **61**, 689 (1989).
[88] L. Segev, A. Salomon, A. Natan, D. Cahen, L. Kronik, F. Amy, C. K. Chan, and A. Kahn, Phys. Rev. B **74**, 165323 (2006).
[89] J. Hwang, E. G. Kim, J. Liu, J. L. Bredas, A. Duggal, and A. Kahn, J. Phys. Chem. C **111**, 1378 (2007).
[90] S. Berkebile, P. Puschnig, G. Koller, M. Oehzelt, F. P. Netzer, C. Ambrosch-Draxl, and M. G. Ramsey, Phys. Rev. B **77**, 115312 (2008).
[91] G. Koller, S. Berkebile, J. Ivanco, F. P. Netzer, and M. G. Ramsey, Surf. Sci. **601**, 5683 (2007).
[92] M. Oehzelt, L. Grill, S. Berkebile, G. Koller, F. P. Netzer, and M. G. Ramsey, ChemPhysChem **8**, 1707 (2007).